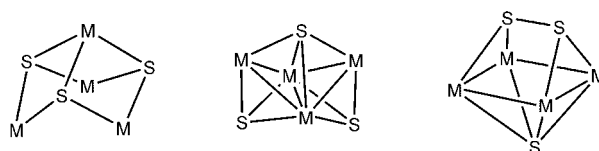


Cluster Compounds

Competing H–H, S–S, and M–M Bond Formation in the “Shape-Shifting” Cluster $[\text{Ru}_4\text{S}_3(\text{arene})_4]^{2+**}$

Matthew L. Kuhlman and Thomas B. Rauchfuss*

Tetrametallic trisulfido clusters^[1] mainly adopt the C_{3v} “Roussin Black salt” structure,^[2,3] illustrated by the classical anion $[\text{Fe}_4\text{S}_3(\text{NO})_7]^-$. This motif has recently attracted interest because M_4S_3 -like fragments comprise the FeMo cofactor in nitrogenase.^[3–5] The only other M_4S_3 structure is the rare C_{2v} capped-butterfly seen in $[\text{Cp}_2\text{Mo}_2\text{Co}_2\text{S}_3(\text{CO})_4]$ ($\text{Cp} = \text{C}_5\text{H}_5$; Scheme 1).^[2] Herein we describe the character-



Scheme 1. Structures of M_4S_3 cluster cores; M–M bonding can vary; left: C_{3v} Roussin Black salt structure, middle: C_{2v} capped-butterfly, and right: face-capped trigonal prism (this work).

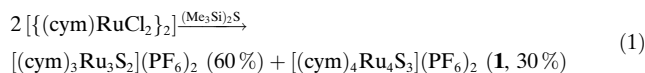
ization of a third M_4S_3 motif; this new cluster is unusual because of its structural dynamics and catalytic properties. In particular, the new M_4S_3 clusters exhibits a previously unobserved competition between S–S and M–M bonding.

[*] M. L. Kuhlman, Prof. Dr. T. B. Rauchfuss
Department of Chemistry
University of Illinois at Urbana-Champaign
Urbana, IL 61801 (USA)
Fax: (+1) 217-333-2685
E-mail: rauchfuz@uiuc.edu

[**] This research was supported by the National Science Foundation. We thank Scott Wilson and Teresa Prussak-Wieckowska for assistance with the X-ray crystallography.

Studies on this dynamic property revealed that the new clusters catalyze the reduction of protons to H_2 .

We have shown that $[(\text{cym})\text{RuCl}_2]_2$ ($\text{cym} = 4\text{-}i\text{PrC}_6\text{H}_4\text{Me}$) reacts with $(\text{Me}_3\text{Si})_2\text{S}$ to produce trigonal bipyramidal $[(\text{cym})_3\text{Ru}_3\text{S}_2]^{2+}$.^[6] We have found that this simple synthesis also affords the previously unrecognized tetrametallic species $[(\text{cym})_4\text{Ru}_4\text{S}_3]^{2+}$ ($\mathbf{1}^{2+}$). The distinctive solubility properties of $[(\text{cym})_4\text{Ru}_4\text{S}_3](\text{PF}_6)_2$ ($\mathbf{1}$) facilitates its easy isolation in 30% yield [Eq. (1)].



In MeCN solution, cluster $\mathbf{1}^{2+}$ is stable at 80°C in the presence of PPh_3 , and it is stable to UV photolysis.^[7]

The reaction stoichiometry leading to $\mathbf{1}^{2+}$ is deceptive: Ru^{II} chlorides are ostensibly converted into the corresponding Ru^{II} sulfides. The ^1H NMR data for $\mathbf{1}^{2+}$ indicate low symmetry, which is incompatible with known M_4S_3 motifs. X-ray crystallographic analysis of $\mathbf{1}$ revealed that the dication adopts a novel structure, described as a face-capped trigonal prism (Figure 1). An equilateral Ru_4 square (Ru-Ru bond $2.81 \pm 0.03 \text{ \AA}$) is capped by $\mu_4\text{-S}$ and $\mu_4\text{-S}_2$ ligands. The crystallographic result shows that $\mathbf{1}^{2+}$ formally arises via an internal reduction of two Ru^{II} to Ru^{I} concomitant with oxidative coupling of two sulfides to persulfide (S_2^{2-}). The 64-electron compound follows the 18 electron rule, although Wade's rules predict a nido cluster (9 electron pair/seven vertex).

The crystallographic analysis reveals that the four isopropyl groups are oriented towards the persulfide-containing face of the Ru_4 square, which is more spacious than the Ru_4S side. A space-filling model indicates steric crowding between the arene substituents,

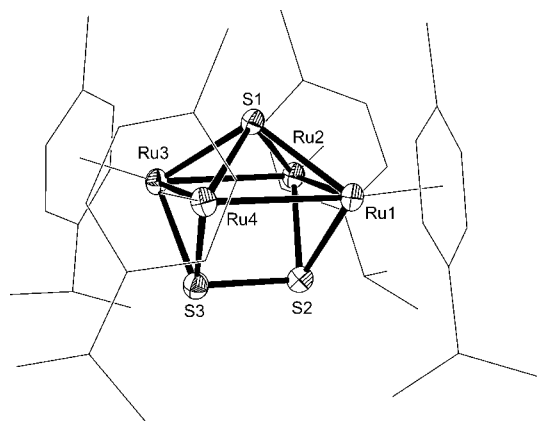


Figure 1. Molecular structure of $\mathbf{1}$. Thermal ellipsoids are set at 50% probability. Select bond lengths [\AA]: Ru1-Ru2 2.782, Ru1-Ru4 2.827, Ru4-Ru3 2.776, Ru2-Ru3 2.848, S1-Ru2 2.352, S3-S2 2.109, S2-Ru2 2.281.

which would lead to restricted rotation about the ruthenium-arene bonds. Indeed, the ^1H NMR spectrum for $\mathbf{1}^{2+}$ is simple at 70°C but becomes complex at lower temperatures as arene rotation is slowed (Figure 2). At -35°C , 13 $\text{CH}_3\text{C}_6\text{H}_4\text{iPr}$ signals are resolved (Figure 2b) 14 $\text{CH}_3\text{C}_6\text{H}_4\text{iPr}$ signals would be consistent with seven possible atropisomers: $(\text{up})_4$, $(\text{down})_4$, $\text{trans}(\text{up})_2(\text{down})_2$, $\text{cis}(\text{up-}\parallel)_2(\text{down-}\parallel)_2$, $\text{cis}(\text{up-}\perp)_2(\text{down-}\perp)_2$, $(\text{up})_3(\text{down})$, and $(\text{up})(\text{down})_3$, where up and down refer to the orientation relative to the S_2 and S faces of the Ru_4 square (see Scheme 2). The number of isomers implies that rotation of the S_2 ligand is slow on the NMR timescale, such that two $\text{cis}(\text{up})_2(\text{down})_2$

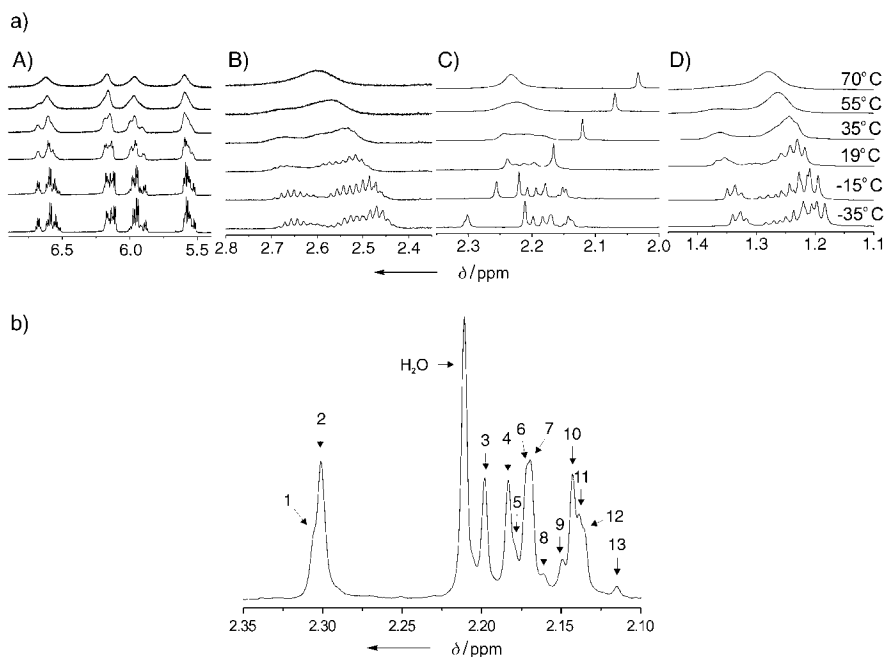
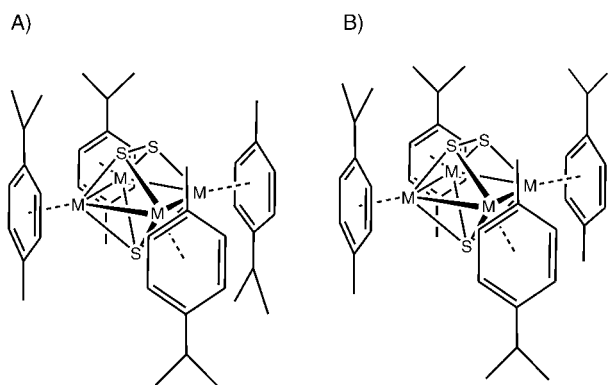


Figure 2. a) Variable temperature ^1H NMR spectra ($[\text{D}_3]\text{MeCN}$) for $\mathbf{1}$ demonstrating restricted rotation of the cym ligands. A) Aromatic region, B) methine (isopropyl), C) methyl, and D) methyl (isopropyl) of cym. b) Expansion of the $\text{CH}_3\text{C}_6\text{H}_4\text{iPr}$ region for the -35°C spectrum, demonstrating the coexistence of several atropisomers.

isomers are implicated, those where the cisoid Me groups are parallel (\parallel ; Scheme 2) or perpendicular (\perp) to the S_2 unit. Restricted rotation of $\eta^6\text{-arene}$ ligands has rarely been detected in mononuclear complexes^[8] and never in a metal cluster. The isomerization barrier could in principle be increased through modifications in the arene ligand.

The cyclic voltammetry (CV) of $\mathbf{1}$ revealed sequential $1 e^-$ reductions at -970 and -1270 mV (not shown; all potentials are referenced to the $\text{Ag}|\text{AgCl}$ couple). A reversible event at 790 mV is assigned to a $2 e^-$ oxidation. Chemical reduction of $\mathbf{1}^{2+}$ with two equivalents of $[\text{Cp}^*\text{Co}]$ ($\text{Cp}^* = \text{C}_5\text{Me}_5$; $E^\circ = 1.73$ versus $\text{Ag}|\text{AgCl}$) yielded the neutral cluster $[(\text{cym})_4\text{Ru}_4\text{S}_3]$ ($\mathbf{2}^0$). The ^1H NMR spectroscopy data for this neutral species revealed a 3:1 ratio for the cym signals, which indicates idealized C_{3v} symmetry as expected for the Roussin motif, which was confirmed crystallographically (Figure 3). In contrast to other Roussin-like clusters, the apical metal atom is not connected to the other three metal centers by M-M



Scheme 2. Structures of two atropisomers of **1**, A) the *cis* || isomer and B) the (up)₃(down) isomer.

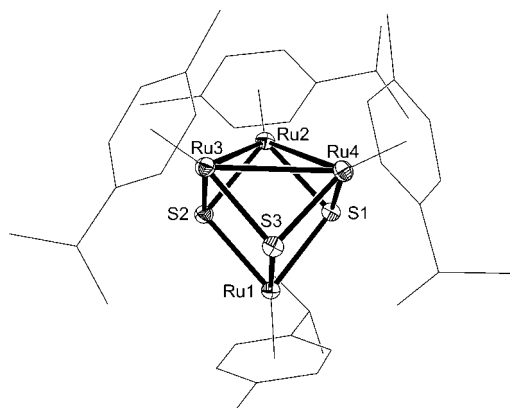
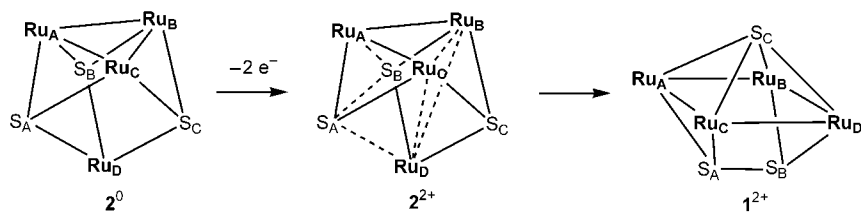


Figure 3. Molecular structure of **2**⁰ with thermal ellipsoids set at 50% probability. Select interatomic distances [Å]: Ru1...Ru2 3.620, Ru3-Ru2 3.079, Ru3-Ru4 3.059, Ru4-Ru2 3.007, Ru1-S2 2.377, Ru2-S2 2.324.

bonds. Two Ru–Ru bonds are expected in a 68e[−] M₄ cluster, thus each of the three comparably elongated Ru–Ru bonds within the Ru₃ basal plane is consistent with a bond order of 2/3. Compound **2**⁰ is formally related to the cubane [(cym)₄Ru₄S₄]^[9,10] by removal of one sulfur atom and subsequent formation of three Ru–Ru bonds.

The scan-rate dependence of the CV of **1** is consistent with a coupled electrochemical–chemical process. The reduction **1**²⁺→**1**⁺ is fully reversible, but the second reduction is not, hence this event is attributed to the rearrangement to the Roussin-like cluster **2**. At slow scan rates (20 mVs^{−1}), the initially generated **2**⁺ is fully converted into **1**⁺, indicated by the event at −970 mV. At faster scan rates (500 mVs^{−1}) separate oxidations are observed for **2**⁰→**2**⁺ and **2**⁺→**2**²⁺. The



Scheme 3. Pathway for the oxidation of **2**⁰.

scan-rate dependence suggests that the rearrangement of **2**⁺ into **1**⁺ occurs with a half-life of approximately 100 ms. A plausible pathway for rearrangement associated with the oxidation of **2**⁰ is shown in Scheme 3.

Reflecting its electron-rich character and the robustness of the Ru–S ensemble, **2**⁰ reacts efficiently with acids, such as HOTf (OTf = [CF₃SO₃][−]), to regenerate **1**²⁺. When this reaction is conducted in CH₂Cl₂ solution, **1**⁺(OTf)₂ crystallizes in near quantitative yield. Interestingly, this reaction occurs with formation of H₂ (¹H NMR: δ = 4.6 ppm in CH₂Cl₂ solution), [Eq. (2)].



Qualitative experiments suggest that **2**⁰ is a two-electron reductant since the addition of one equivalent of HOTf precipitates an approximately 50% yield of **1**⁺(OTf)₂. Thus, the implied monohydride intermediate **2H**⁺ is apparently more reactive towards HOTf than **2**⁰. Since **2**⁰ is capable of reducing protons and **1**²⁺ undergoes efficient reduction, a catalytic cycle is apparent, but the CV results were unexpected. Indeed with HOTs a catalytic current that correlates with [HOTs] is observed, but not at the expected potential of approximately *i*_{cat} = −1 V. Instead *i*_{cat} emerges in the range −0.80 to −0.60 V (Figure 4). The two new reduction events

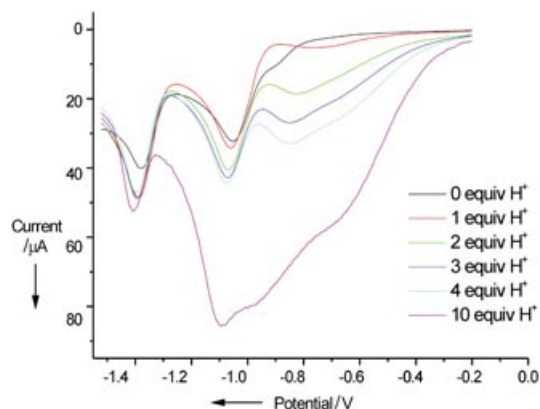


Figure 4. Voltammograms of 10^{−3} M **1** in 0.1 M Bu₄NPF₆ MeCN solution. The reductive current at approximately −800 mV can be seen to correlate with the [*p*-MeC₆H₄SO₃H]. Conditions: scan rate = 100 mVs^{−1}, Pt wire counter electrode, a glassy carbon electrode working electrode, Ag/AgCl reference.

observed in presence of H⁺ suggest that **1**²⁺ forms an electroactive protonated derivative, although we were unable to spectroscopically detect such a species. The two new reduction events not only increase in current with increasing [H⁺], but shift to a more negative potential with increasing [H⁺], as seen in catalytic systems.^[11,12]

In summary, new M₄S₃ clusters have been shown to exhibit “shape-shifting”, involving redox- and proton-induced conversions between C_{3v} and trigonal-prismatic structures. The parent cationic cluster is further unusual in that its arene

ligands exhibit restricted rotation owing to steric compression. The work underscores the promise of metal sulfide ensembles for hydrogen processing.

Experimental Section

1: A stirred suspension of (4.160 g, 6.8 mmol) of $[(\text{cym})\text{RuCl}_2]^{[13]}$ in warm THF (150 mL) was treated with (2.14 mL, 10.2 mmol) of $(\text{Me}_3\text{Si})_2\text{S}$. The solid slowly dissolved followed by formation of a brown precipitate. The slurry was stirred at 50 °C for 1 h. The solid was collected by filtration and washed with THF (20 mL). The dried brown powder was extracted into H_2O (100 mL) this solution was treated with KPF_6 (2.50 g 13.3 mmol) to precipitate a mixture of $[(\text{cym})_3\text{Ru}_3\text{S}_2](\text{PF}_6)_2$ and **1**. After washing this solid with CH_2Cl_2 to remove $[(\text{cym})_3\text{Ru}_3\text{S}_2](\text{PF}_6)_2$, the residue was extracted into acetone, and this solution was concentrated to 5 mL. Addition of Et_2O (80 mL) precipitated a brown powder. Yield: 1.34 g (30%). $^1\text{H NMR}$ (500 MHz, $[\text{D}_3]\text{MeCN}$): 1.28 (m, 6H), 2.22 (m, 3H), 2.61 (m, 1H), 6.61 (m, 1H), 6.14 (m, 1H), 5.96 (m, 1H), 5.59 ppm (m, 1H). ESI-MS: m/z 519 ($[\text{M}^{2+}]$). Elemental analysis (%) calcd for $\text{C}_{40}\text{H}_{56}\text{F}_{12}\text{P}_2\text{Ru}_4\text{S}_3$: C 36.19, H 4.25, N 0; found: C 35.74, H 4.15, N 0.28.

2^o: A solution of $[\text{Cp}^*\text{Co}]$ (424 mg, 1.29 mmol) in THF (40 mL) was added to a stirred solution of **1** (814 mg 0.61 mmol) in MeCN (130 mL). After 1 h, the solvent was removed in vacuo, and the resulting red powder was extracted with hexane (50 mL). Dark red crystals were obtained upon concentrating and cooling the solution. Yield: 464 mg (65%). $^1\text{H NMR}$ (500 MHz, $[\text{D}_8]\text{THF}$): 1.22 (d, $J = 7$ Hz, 6H), 1.37 (d, $J = 7$ Hz, 18H), 1.78 (s, 3H), 2.34 (s, 9H) 2.58 (sept, $J = 7$ Hz, 1H) 2.78 (sept, $J = 7$ Hz, 3H) 4.13 (d, $J = 6$ Hz, 2H) 4.47 (d, $J = 6$ Hz, 2H) 4.80 (d, $J = 6$ Hz, 6H) 4.97 ppm (d, $J = 6$ Hz, 6H). Elemental analysis (%) calcd for $\text{C}_{40}\text{H}_{56}\text{Ru}_4\text{S}_3$: C 46.31, H 5.44, N 0; found: C 46.48, H 5.45, N 0.17.

Crystallography: Data was collected at -78°C on a Siemens Platform/CCD automated diffractometer. Data processing was performed with SAINT PLUS version 6.22. Structures were solved using direct methods and refined using full-matrix least-squares on F^2 using Bruker SHELXTL version 6.10. Hydrogen atoms were fixed in idealized positions with thermal parameters $1.5 \times$ those of the attached carbon atoms. The data were corrected for absorption on the basis of ψ -scans. CCDC-244393 and CCDC-244394 contain the supplementary crystallographic data for this paper. These data can be obtained free of charge via www.ccdc.cam.ac.uk/conts/retrieving.html (or from the Cambridge Crystallographic Data Centre, 12 Union Road, Cambridge CB21EZ, UK; fax: (+44) 1223-336-033; or deposit@ccdc.cam.ac.uk).

Received: July 10, 2004

Keywords: arenes · hydrogen · rearrangement · ruthenium · sulfur

- [1] J. R. Long, R. H. Holm, *J. Am. Chem. Soc.* **1994**, *116*, 9987.
- [2] M. D. Curtis, P. D. Williams, W. M. Butler, *Inorg. Chem.* **1988**, *27*, 2853.
- [3] D. Coucouvanis, J. Han, N. Moon, *J. Am. Chem. Soc.* **2002**, *124*, 216.
- [4] S. C. Lee, R. H. Holm, *Proc. Natl. Acad. Sci. USA* **2003**, *100*, 3595.
- [5] S. C. Lee, R. H. Holm, *Chem. Rev.* **2004**, *104*, 1135.
- [6] J. R. Lockemeyer, T. B. Rauchfuss, A. L. Rheingold, *J. Am. Chem. Soc.* **1989**, *111*, 5733.
- [7] A. L. Ecker mann, D. Fenske, T. B. Rauchfuss, *Inorg. Chem.* **2001**, *40*, 1459.
- [8] M. Nambu, D. L. Mohler, K. Hardcastle, K. K. Baldrige, J. S. Siegel, *J. Am. Chem. Soc.* **1993**, *115*, 6138.

- [9] H. Seino, Y. Mizobe, M. Hidai, *New J. Chem.* **2000**, *24*, 907.
- [10] M. Hidai, S. Kuwata, Y. Mizobe, *Acc. Chem. Res.* **2000**, *33*, 46.
- [11] I. Bhugun, D. Lexa, J.-M. Savéant, *J. Am. Chem. Soc.* **1996**, *118*, 3982.
- [12] F. Gloaguen, J. D. Lawrence, T. B. Rauchfuss, *J. Am. Chem. Soc.* **2001**, *123*, 9476.
- [13] M. A. Bennett, A. K. Smith, *J. Chem. Soc. Dalton Trans.* **1974**, 233.